



Research article

Electrochemical reduction of CO₂ using Germanium-Sulfide-Indium amorphous glass structuresF.S. Khan^{a,*}, M. Sugiyama^a, K. Fujii^b, Yu.S. Tver'yanovich^c, Y. Nakano^d^a Department of Advanced Interdisciplinary Studies, School of Engineering, University of Tokyo, Japan^b RIKEN Center for Advanced Photonics, Wako, Japan^c Institute of Chemistry, St. Petersburg State University, Russia^d Department of Electrical Engineering, School of Engineering, University of Tokyo, Japan

ARTICLE INFO

Keywords:

Chemical engineering

Energy

Materials chemistry

Materials application

Electrochemistry

CO₂ reduction

Chalcogenides

Electrocatalysis

Carbon monoxide

Formic acid

Carbon paper

ABSTRACT

The research in electrochemical reduction of CO₂ is shifting towards the discovery of new and novel materials. This study shows a new class of material, that of Ge-S-In chalcogenide glass, to be active for reduction of CO₂ in aqueous solutions. Experiments were conducted with bulk and particle form of the material, yielding different product for each structural form. Faradaic efficiency of upto 15% was observed in bulk form for CO production while formic acid with up to 26.1 % faradaic efficiency was measured in powder form. Chalcogenide studies have focused primarily on the photoelectrochemical reduction however these results provide a strong merit for introducing metal in chalcogenide glass structures for electrochemical reduction of CO₂. The activity for CO₂ reduction and the change in product selectivity reflects that further efforts to improve the glass structures can be undertaken in order to increase the faradaic efficiency and selectivity of the products.

1. Introduction

During the last century, CO₂ emissions have risen to an alarming rate which has caused an uptick in research focusing on the utilization of CO₂. Such studies can help to achieve two important targets: the storage of excess energy from renewable sources and an avenue for mitigating CO₂ from the atmosphere [1].

In order to achieve a viable solution for the preceding targets, researchers have tried various methods but the most common has been the solar-powered electrochemical and photoelectrochemical reduction of CO₂. Development of electrodes that can effectively convert CO₂ into valuable products such as CO, HCOOH, CH₄ etc has been the main focus of such efforts [2].

Initial research in the field of working electrodes had focused on bulk metals however in recent years, researchers have diverted their attention towards new and novel structures. One such recent example is of iodide-derived nanostructured Ag catalysts that can efficiently reduce CO₂ to CO with more than 94% faradaic efficiency (FE) [3].

Transition-metal chalcogenides (TMCs) have also attracted considerable interest because of their electrochemical and mechanical

properties [4, 5]. Examples include WSe₂ which has been reported to produce CO with upto 24% faradaic efficiency (FE) [6] and ZnTe, which has been shown to have a 22% FE towards CO production [7]. Sulfides in particular have been of interest and as a representative material, MoS₂ has been widely reported as an efficient catalyst for hydrogen evolution and oxygen reduction while also being active towards CO₂ reduction [8, 9]. Recently, sulfur doped indium catalyst has been reported to be extremely active towards formic acid production with FE of more than 85% and high current density [10]. Other sulfide materials such as CdS and ZnS have also been shown to produce CO during CO₂ reduction [11, 12].

The morphology and the nature of such materials has been one of the key frontiers of research in this field [13] and use of semiconducting germanium-based metal sulfide glassy structures has never been attempted. Glass structures consists of local defects, which can potentially act as reaction centers for CO₂-reduction while the low mobility in chalcogenide glasses can also possibly assist in accumulating electrons along the structural defects and aid in catalyzing electron-intensive reduction processes. Indium metal has already been extensively used for electrochemical conversion of CO₂ into formic acid [14, 15] while the

* Corresponding author.

E-mail address: fahd@hotaka.t.u-tokyo.ac.jp (F.S. Khan).

sulfide atoms have shown to increase the catalytic activity [16, 17]. Attempting to combine such qualities, germanium-sulfide-indium chalcogenide glass was chosen as the heterogeneous electrode material for the electrochemical reduction of CO₂.

In addition to the bulk phase, particle form of the same chalcogenide glass was tested for CO₂RR in order to make a comparative assessment with the bulk phase. Carbon fiber paper (CP) was employed as the substrate for particle chalcogens. CP was chosen because of its composite of carbon and carbon fibers, which apart from being conductive, also allow cheaper price than glassy carbon substrates while offering enhanced structural rigidity than carbon cloth [18].

2. Experimental

Samples of chalcogenide glasses with the general formula (1-x)GeS_{1.5}(x)In were prepared. Indium concentration (x) was chosen to be 0.01, 0.1, 0.4, 0.5, 0.6, 0.12. To fabricate such glass compositions, the respective weighed quantities of germanium, sulfur and indium were vacuumed in quartz ampoules and heated to the temperature of the melting point of sulfur. The synthesis was carried out under a gradual temperature increase in a rocking furnace up to 1100 K; the ampoules were then held for 8 h and subsequently cooled in air.

Home-made H-type leak-tight electrochemical cells were used for CO₂ reduction, with 100 cm³ volume and 70 mL of electrolyte. Experiments were conducted for at least 45 min and the end-products were collected for further analysis. The working and reference electrodes were put in the same compartment and separated from the counter electrode by a nafion film (DuPont: N117). Ag/AgCl was employed as the reference electrode. A working device for the reduction of CO₂ requires a source of protons

and electrons and so platinum was used for the oxygen evolution reaction (OER), which served as the other half-reaction for this purpose: $2\text{H}_2\text{O} \rightarrow 4\text{H}^+ + 4\text{e}^- + \text{O}_2$. 0.5 M KHCO₃ electrolyte was used and saturated with CO₂ to obtain a pH of 7.1 in the cathode. Same electrolyte was used in the anode chamber. The pH changes were not observed during the experiment. Since CO₂ reduction is a redox reaction, during CO₂RR, O₂ evolution takes place at the counter electrode and so the separation between the working and counter electrodes helps to ensure that the recombination of the products produced on these two electrodes can be effectively prohibited. The gas product was then sampled manually through syringe using HP Agilent 7890 Gas Chromatographer (GC). The liquid phase products were determined by Ion Chromatography (IC) and collected with a Thermo Scientific Dionex ICS-5000 system. The energy dispersive electron (EDX) spectroscopy was employed to obtain the elemental analysis of the samples. The X-ray emission photoelectron spectroscopy was conducted by Al X-ray source in ULVAC-PHI 1600C to analyze the surface layer. PHI Multipak software was used to obtain the curve-fitting spectra. Electrochemical experiments were performed using Solartron 1280C potentiostat while a stir bar was used within the electrochemical cell. Electrodes were prepared by affixing a copper wire to an indium contact on the bulk surface. The exposed portion of the copper wire was also covered with indium using a solder. Indium contact acts as an ohmic contact between the metal and semiconductor. The exposed indium was then covered with epoxy to avoid any interaction between the electrolyte and the ohmic contact. For the particle-based electrode, the bulk sample was crushed to micron size particles. A solution was prepared with ethanol as the solvent and nafion as the adhesive material along with the crushed particles in the ratio 30:5:1, respectively. 2 mg/cm² was chosen as the loading amount onto the CP substrate. The mixed solution was

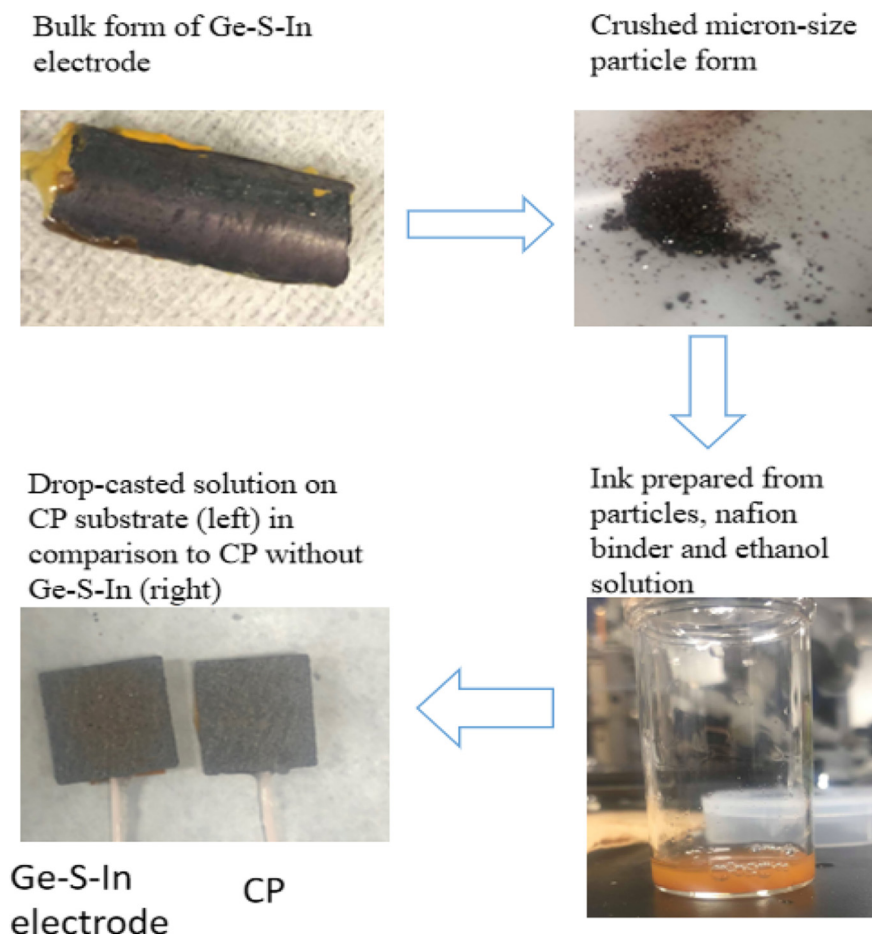


Figure 1. Preparation of samples from bulk to particle form.

Table 1. Elemental analysis of the bulk samples by EDX.

Element	Weight %	Atomic %	Error %
Oxygen	1.57	4.88	0.36
Sulfur	34.72	53.91	0.17
Germanium	53.86	36.94	0.24
Indium	9.86	4.27	0.68
	100.00	100.00	

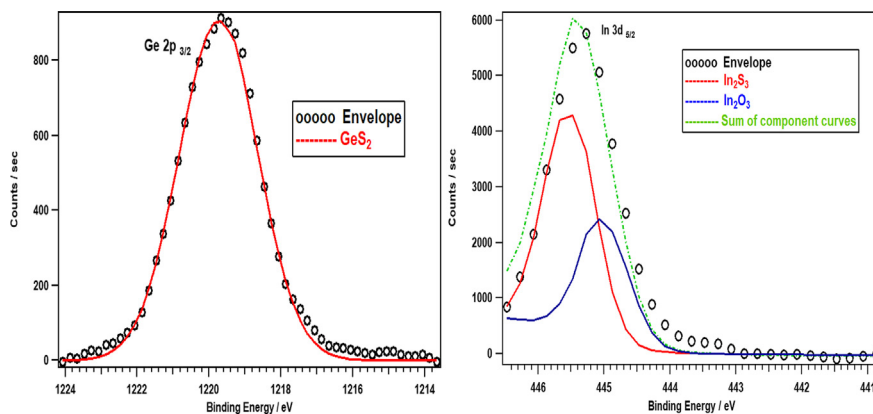


Figure 2. Fitted XPS spectra of Ge (left) and In (right), indicating that the surface is predominantly made up of metal sulfides; GeS₂ and In₂S₃ with smaller presence of In₂O₃.

treated ultrasonically for 30 min to form a homogeneous ink. A 50 μl solution was then drop casted onto 1 cm² of carbon paper, which acted as a substrate. Copper wire was connect to the substrate and exposed copper was covered with epoxy. Figure 1 shows the different stages of this electrode preparation. The electrolyte was purged with CO₂ or Ar for 25 min prior to experimental or control trials, respectively.

3. Result and discussion

The characterization of the amorphous Ge-S-In chalcogenide glass was carried out using EDX spectroscopy [19, 20, 21, 22], which has an analysis depth of upto 2 μm. The elemental composition of the sample is shown in Table 1. Oxygen poisoning was seen, which is a common occurrence during furnace fabrication processes. Sulfur deficiencies have also been observed in amorphous chalcogenide glasses [23]. XPS analysis was conducted since it has a depth resolution of 5–10 nm, which helps in

analyzing the surface layer and identification of oxidation states. The XPS peaks were assigned [24] using the references available on the online NIMS database for XPS spectra. The curve-fitted XPS spectra in Figure 2, identify the presence of GeS₂ [25] and In₂S₃ [26] along with In₂O₃ [27] on the surface. Thus, the surface layer of the chalcogenide glass structure consisted of sulfides [28] along with minor presence of In₂O₃. The photo-response for the chalcogenide glass was measured by excitation spectroscopy at room temperature however the samples did not exhibit any reaction to the blue laser light (corresponding to its band gap potential), possibly due to the amorphous nature of the structure. In non-crystalline structures [29, 30], the recombination rate has been observed to be high which causes the photo-response of such samples to suffer.

Samples with 5% In concentration were selected for the electrochemical reduction of CO₂ because of flatter surfaces. The response of the samples in the inert Ar saturated electrolyte was compared to the CO₂ saturated electrolyte. As can be seen in Figure 3, the bulk sample started to exhibit a slightly higher current density in CO₂ saturated electrolyte at

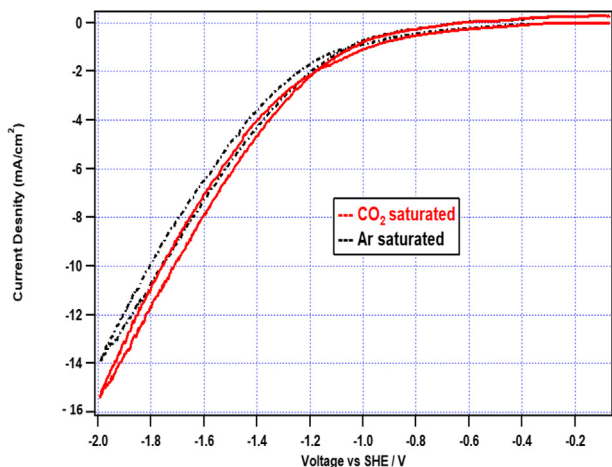


Figure 3. IV response of the bulk-based electrode in CO₂-(red) and Ar-(black) saturated electrolyte.

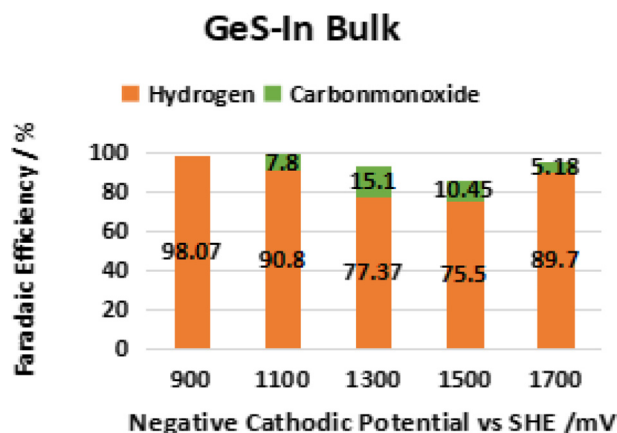


Figure 4. Faradaic Efficiency against negative cathodic potentials for bulk samples.

the same negative cathodic potentials, which reflected activity towards the electrochemical reduction of CO₂. The applied cathodic potential range for the CO₂RR experiments was selected on the basis of this enhanced activity observed from the comparative IV graph in Figure 3. Highest faradaic efficiency (FE) of CO was observed to be 15.1 % at -1300 mV vs SHE and the FE for all the potentials are plotted in Figure 4. The samples were also tested for multiple time duration at the best performing potential of -1300 mV vs SHE to confirm the stability of the electrode. The extended use of sample at -1300 mV for almost 5 h and charge transfer of 80 C, confirmed the FE of around 15% for CO production (as can be seen in Figure 5).

It was observed that the maximum current density for stable operation of the samples was 5 mA/cm² beyond which a brown layer, reflecting surface degradation, was observed. This surface poisoning was seen in experiments where the applied potential was more negative than -1500 mV vs SHE. The brown layer could be subsequently removed after cleaning with a strong oxidizing agent such as sulfuric acid. Chalcogenide glasses are stable in acids [31] but oxides have been observed to be reactive in acidic conditions and thus the surface degradation at very negative potentials can be accounted as metal oxide and CO₂RR experiments at those potentials should be avoided. The impedance of the sample was measured to be about 10⁷ ohms (Figure 6).

In comparison to the bulk-based electrode, the particle phase of the samples showed a different response during CO₂RR experiments. The preparation of the CP-supported particle-based electrode was carried out by crushing the bulk sample into micron size particles in order to lower the series resistance in the lateral direction and increase the low coordination sites (corners, steps and kinks). The IV response of the particle-based electrode in CO₂-saturated and Ar-saturated electrolytes is shown in Figure 7. In comparison to the IV response of bulk-based electrode (Figure 3), particle-based electrode reflected higher current density in CO₂-saturated electrolyte, which is an indication of higher CO₂RR activity [32] and confirmed that the change in structural form leads to different IV response.

Figure 8 shows the faradaic efficiency difference between electrodes with and without Ge-S-In. CO evolution observed during use of bulk-based electrodes was almost non-existent in particle-based electrodes. However, formic acid with FE of upto 26.1% was observed. The extended use of the electrode at -1503 mV vs SHE can be seen in Figure 9 where the FE towards formic remained above 25% after a passage of more than 80 C. Increased surface coverage by H ions and intermediate species during CO₂RR experiments have been reported to impact the evolution of products [33]. Formic acid was also observed from experiments conducted with CP-based control electrodes that did not have chalcogenide particles. However, the maximum FE was only 7.1%. The higher FE towards formic acid observed from the particle-based electrode can thus be associated with the presence of chalcogenide particles.

The change in product selectivity between bulk-based and particle-based electrodes is due to the difference in reduction mechanism. This

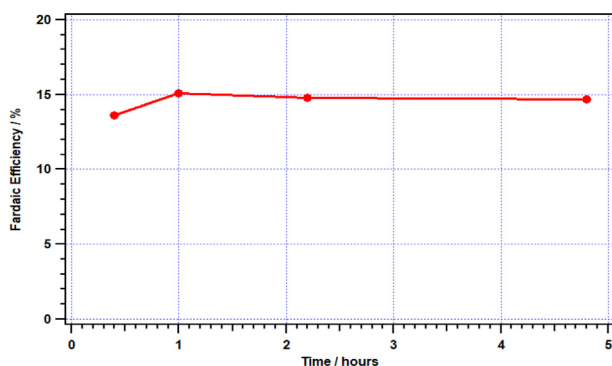


Figure 5. Faradaic Efficiency of CO at extended use of electrode at -1300 mV vs SHE.

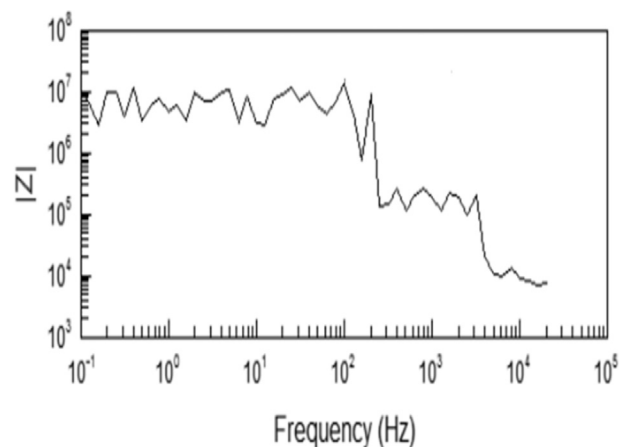


Figure 6. Impedance measurement.

change in mechanism originates from the difference in local electrode structure and activity, which in turn affects the local chemical kinetics [34]. The generally agreed first step in the reduction mechanism for CO₂RR [35] is considered to be the formation of radical CO₂ at the active sites. Subsequently, the reduction direction on the bulk-based and particle-based electrodes take different routes since the binding energies for the intermediate species should differ on the bulk glass surface and CP-supported particle surface. CO production occurs primarily through a key carbon-bound intermediate, COOH, while formic production proceeds through a key oxygen-bound intermediate, OCHO [36]. In view of the products observed during CO₂RR experiments, we theorize that bulk-based electrodes show more propensity to the carbon-bound intermediate, while the oxygen-bound intermediate binds more strongly with the CP-supported particle-based electrode. It has been previously reported [37, 38] that particle catalysts increase the low-coordinated sites (corners, steps and kinks) and this leads to higher activity and shifts in product selectivity. This corresponded to our observation of enhanced CO₂RR activity on particle-based electrode compared to the bulk-based electrode for the same cathodic potentials. Since CP-based control electrode had produced formic acid with upto 7% FE, we speculate that the presence of chalcogenide particles allowed enhancement of bidentate adsorption and thus increased formic acid yields. This is in agreement with the study by Norskov *et al.* [39] where it was suggested that the presence of heterogeneous catalysts on substrate surfaces can aid in further enhancing the adsorption of intermediate species. Hence, it is our hypothesis that the structural differences between bulk-based electrode and CP-supported particle-based electrode cause difference in

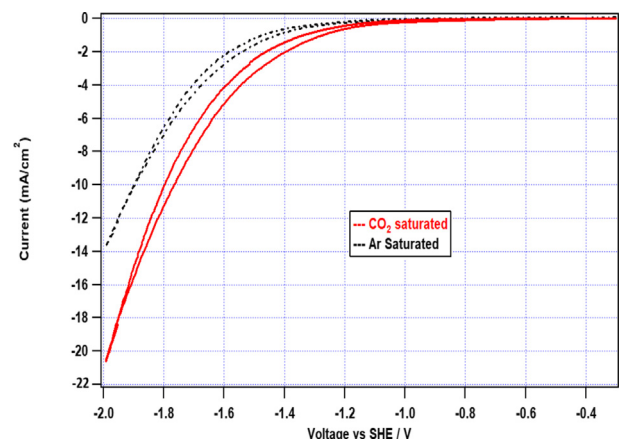


Figure 7. IV response of the CP-supported particle electrode in CO₂-(red) and Ar-(black) saturated electrolyte.

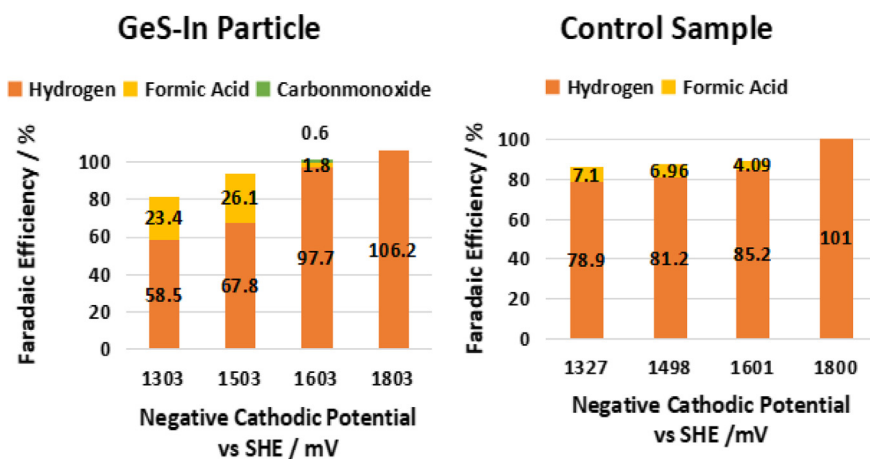


Figure 8. Faradaic Efficiency against negative cathodic potential for particle-based electrode (left) and control electrode (without Ge-S-In particles) (right).

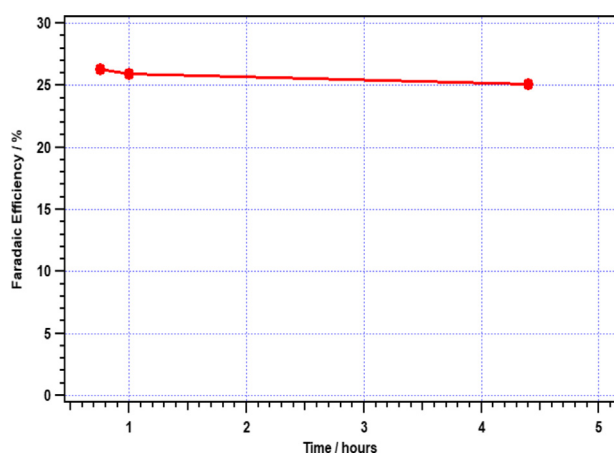


Figure 9. Faradaic efficiency of formic acid at extended use of CP-supported particle electrode at -1503 mV vs SHE.

reaction activity and impact the binding energies for key intermediates to the active sites, thus allowing the change in product selectivity.

4. Conclusion

This study presents a merit for using new class of materials in the research for electrochemical reduction of CO_2 . Germanium-Sulfide-Indium chalcogenide glass material, to the best of our knowledge, has been used for the first time for electrochemical CO_2 reduction. The product selectivity was significantly changed between the bulk and particle form. The melt quenching fabrication method for the production of bulk Ge-S-In allows a cheaper alternative for industrial level fabrication of such materials. Additionally, the difference in product selectivity due to the change of form presents a merit for further investigation into the use of chalcogenide-based glass electrodes.

Declarations

Author contribution statement

F. S. Khan: Conceived and designed the experiments; Performed the experiments; Analyzed and interpreted the data; Wrote the paper.

M. Sugiyama: Conceived and designed the experiments; Analyzed and interpreted the data.

K. Fujii, Yu. S. Tver'yanovich & Y. Nakano: Analyzed and interpreted the data.

Funding statement

This research did not receive any specific grant from funding agencies in the public, commercial, or not-for-profit sectors.

Competing interest statement

The authors declare no conflict of interest.

Additional information

No additional information is available for this paper.

References

- [1] M. Cokoja, C. Bruckmeier, B. Rieger, W.A. Herrmann, F.E. Kühn, Transformation of carbon dioxide with homogeneous transition-metal catalysts: a molecular solution to a global challenge? *Angew Chem. Int. Ed. Engl.* 50 (2011) 8510–8537.
- [2] S.N. Habisreutinger, L. Schmidt-Mende, J.K. Stolarczyk, Photocatalytic reduction of CO_2 on TiO_2 and other semiconductors, *Angew Chem. Int. Ed. Engl.* 52 (2013) 7372–7408.
- [3] Y. Zhang, L. Ji, W. Qiu, X. Shi, A.M. Asiri, X. Sun, Iodide-derived nanostructured silver promotes selective and efficient carbon dioxide conversion into carbon monoxide, *Chem. Commun.* 54 (2018) 2666–2669.
- [4] S.Z. Butler, S.M. Hollen, L. Cao, Y. Cui, J.A. Gupta, H.R. Gutierrez, T.F. Heinz, S.S. Hong, J. Huang, A.F. Ismach, E. Johnston-Halperin, M. Kuno, V.V. Plashnitsa, R.D. Robinson, R.S. Ruoff, S. Salahuddin, J. Shan, L. Shi, M.G. Spencer, M. Terrones, W. Windl, J.E. Goldberger, Progress, challenges, and opportunities in two-dimensional materials beyond graphene, *ACS Nano* 7 (2013) 898–2926.
- [5] M. Xu, T. Liang, M. Shi, H. Chen, Graphene-like two-dimensional materials, *Chem. Rev.* 113 (2013) 3766–3798.
- [6] M. Asadi, K. Kim, C. Liu, P. Philips, Nanostructured transition metal dichalcogenide electrocatalysts for CO_2 reduction in ionic liquid, *Science* 353 (2016) 467–470.
- [7] J. Jang, S. Cho, G. Magesh, Y. Jang, J. Kim, W. Kim, J. Seo, S. Kim, K. Lee, J. Lee, Aqueous-solution route to zinc telluride films for application to CO_2 reduction, *Angew. Chem. Int. Ed.* 53 (2014) 5852–5857.
- [8] M. Asadi, B. Kumar, A. Behranginia, B.A. Rosen, A. Baskin, N. Repnin, D. Pisasale, P. Philips, W. Zhu, R. Haasch, R.H. Klie, P. Karl, J. Abiade, A. Salehi-Khonjin, Robust carbon dioxide reduction on molybdenum disulphide edges, *Nat. Commun.* 5 (2014) 4470–4478.
- [9] X. Cui, G.H. Lee, Y.D. Kim, G. Arefe, P.Y. Huang, C.H. Lee, D.A. Chenet, X. Zhang, L. Wang, F. Ye, F. Pizzocchero, B.S. Jessen, K. Watanabe, T. Taniguchi, D.A. Muller, T. Low, P. Kim, Multi-terminal transport measurements of MoS_2 using a van der Waals heterostructure device platform, *Nat. Nanotechnol.* 10 (2015) 534–540.
- [10] W. Ma, S. Xie, X. Zhang, F. Sun, J. Kang, Z. Jiang, Q. Zhang, D. Wu, Y. Wang, Promoting electrocatalytic CO_2 reduction to formate via sulfur-boosting water activation on indium surfaces, *Nat. Commun.* 10 (2019) 892–901.
- [11] J. Shi, D. Shao, J. Zhang, D. Tan, X. Tan, B. Zhang, B. Han, F. Zhang, L. Liu, X. Chengab, Highly selective and efficient reduction of CO_2 to CO on cadmium electrodes derived from cadmium hydroxide, *Chem. Commun.* 54 (2018) 5450–5453.
- [12] M. Kanemoto, H. Hosokawa, Y. Wada, K. Murakoshi, S. Yanagida, T. Sakata, H. Mori, M. Ishikawa, H. Kobayashi, Semiconductor photocatalysis. Part 20. Role of surface in the photoreduction of carbon dioxide catalyzed by colloidal ZnS nanocrystallites in organic solvent, *J. Chem. Soc., Faraday Trans.* 92 (1996) 2401–2411.

- [13] J. White, M. Baruch, J. Pander III, Y. Hu, I. Fortmeyer, J. Park, T. Zhang, K. Liao, J. Gu, Y. Yan, T. Shaw, E. Abelev, A. Bocarsly, Light-driven heterogeneous reduction of carbon dioxide: photocatalysts and photoelectrodes, *Chem. Rev.* 115 (2015) 12888–12935.
- [14] S. Kapusta, N. Hackerman, The electroreduction of carbon dioxide and formic acid on tin and indium electrodes, *J. Electrochem. Soc.* 130 (1983) 607–613.
- [15] Z. Xia, M. Freeman, D. Zhang, B. Yang, L. Lei, Z. Li, Y. Hou, Highly selective electrochemical conversion of CO₂ to HCOOH on dendritic indium foams, *ChemElectroChem* 5 (2018) 253–258.
- [16] G. Li, D. Zhang, Q. Qiao, Y. Yu, D. Peterson, A. Zafar, R. Kumar, S. Curtarolo, F. Hunte, S. Shannon, Y. Zhu, W. Yang, L. Cao, All the catalytic active sites of MoS₂ for hydrogen evolution, *J. Am. Chem. Soc.* 138 (2016), 16632–16633.
- [17] H. Li, C. Tsai, A. Koh, L. Cai, L.L. Contryman, A.W. Fragapane, A.H. Zhao, J. Han, H.S. Manoharan, H.C. Abild-Pedersen, F. Nørskov, J.K. Zheng, Activating and optimizing MoS₂ basal planes for hydrogen evolution through the formation of strained sulphur vacancies, *Nat. Mater.* 15 (2016) 48–53.
- [18] A. Lucas-Consuegra, J. Serrano-Ruiz, N. Gutiérrez-Guerra, J. Valverde, Low-temperature electrocatalytic conversion of CO₂ to liquid fuels: effect of the Cu particle size, *Catalysts* 8 (2018) 340–351.
- [19] A. Kassim, H. Min, L. Siang, S. Nnglingam, Sem, edax and uv-visible studies on the properties of Cu₂S thin films, *Chalcogenide Lett.* 8 (2011) 405–410.
- [20] S.M. Ho, Application of energy dispersive X-ray analysis technique in chalcogenide metal thin films: review, *Middle East J. Sci. Res.* 24 (2016) 445–449.
- [21] P. Yuan, A. Wang, X. Luo, Y. Xue, L. Zhang, J. Feng, A novel electrochemical immunosensor for highly sensitive detection of prostate-specific antigen using 3D open-structured PtCu nanoframes for signal amplification, *Biosens. Bioelectron.* 126 (2019) 187–192.
- [22] L. Zhang, X. Fang, Z. Xue, L. Chen, A. Wang, D. Han, Z. Wang, J. Feng, Facile solvothermal synthesis of Pt₇₁Co₂₉ lamellar nanoflowers as an efficient catalyst for oxygen reduction and methanol oxidation reactions, *J. Colloid Interface Sci.* 536 (2019) 556–562.
- [23] D. Hewak, D. Brady, R. Curry, Chalcogenide glasses for photonics device applications, in: G.S. Murggan (Ed.), *Photonic Glasses and Glass-Ceramics*, Research Signpost, Kerala, 2010, pp. 29–102.
- [24] I. Kusunoki, M. Sakai, Y. Igari, S. Ishidzuka, T. Takami, T. Takaoka, M. Nishitani-Gamo, T. Ando, XPS study of nitridation of diamond and graphite with a nitrogen ion beam, *Surf. Sci.* 492 (2001) 315–328.
- [25] W. Morgan, J. Van Wazer, Binding energy shifts in the x-ray photoelectron spectra of a series of related Group IVa compounds, *J. Phys. Chem.* 77 (1973) 964–969.
- [26] C. Battistoni, L. Gastald, A. Lapicciarella, G. Mattogno, C. Viticoli, Octahedral vs tetrahedral coordination of the Co(II) ion in layer compounds: Co_xZn_{1-x}In₂S₄ (0 < x < 0.46) solid solution, *J. Phys. Chem. Solid.* 47 (1986) 899–903.
- [27] L. Kazmerski, O. Jamjoum, P. Ireland, S. Deb, R. Mickelsen, W. Chen, Summary abstract: oxidation of CuInSe₂, *J. Vac. Sci. Technol.* 19 (1982) 467–486.
- [28] Z. Boncheva-Mladenova, Z.G. Ivanova, A Study of glass phases of the germanium-sulphur-indium system, *J. Non-Cryst. Solids* 30 (1978) 147–153.
- [29] D. Chekulaev, V. Garber, A. Kaplan, Free carrier plasma optical response and dynamics in strongly pumped silicon nanopillars, *J. Appl. Phys.* 113 (2013) 143101.
- [30] R.A. Sinton, R.M. Swanson, Recombination in highly injected silicon, *IEEE Trans. Electron Devices* ED 34 (1987) 1380–1389.
- [31] M.J. Manos, C.D. Malliakas, M.J. Kanatzidis, Heavy-metal-ion capture, ion-exchange, and exceptional acid stability of the open-framework chalcogenide (NH₄)₄In(12)Se(20), *Chemistry* 13 (2007) 51–58.
- [32] F. Li, H. Zhang, S. Ji, W. Liu, D. Zhang, C. Zhang, J. Yang, F. Yang, L. Lei, High performance Sn-in cathode for the electrochemical reduction of carbon dioxide to formic acid, *Int. J. Electrochem. Sci.* 14 (2019) 4161–4172.
- [33] K. Kuhl, E. Cave, D. Abram, T. Jaramillo, New insights into the electrochemical reduction of carbon dioxide on metallic copper surfaces, *Energy Environ. Sci.* 20 (2012) 7050–7059.
- [34] D. Raciti, M. Mao, J.H. Park, Chao Wang, Low-overpotential electroreduction of carbon monoxide using copper nanowires, *J. Electrochem. Soc.* 165 (2018) F799–F804.
- [35] K.J.P. Schouten, Y. Kwon, C.J.M. van der Ham, Z. Qin, M.T.M. Koper, A new mechanism for the selectivity to C1 and C2 species in the electrochemical reduction of carbon dioxide on copper electrodes, *Chem. Sci.* 2 (2011) 1902.
- [36] J. Feaster, C. Shi, E. Cave, T. Hatsukade, D. Abram, K. Kuhl, C. Hahn, J. Nørskov, T. Jaramillo, Understanding selectivity for the electrochemical reduction of carbon dioxide to formic acid and carbon monoxide on metal electrodes, *ACS Catal.* 7 (2017) 4822–4827.
- [37] R. Reske, H. Mistry, F. Behafarid, B.R. Cuenya, P. Strasser, Particle size effects in the catalytic electroreduction of CO₂ on Cu nanoparticles, *J. Am. Chem. Soc.* 136 (2014) 6978–6986.
- [38] O. Baturina, Q. Lu, M. Padilla, X. Le, W. Li, A. Serov, K. Artyushkov, P. Atanassov, F. Xu, A. Epshteyn, T. Brintlinger, M. Schuett, G. Collins, CO₂ electroreduction to hydrocarbons on carbon-supported Cu nanoparticles, *ACS Catal.* 4 (2014) 3682–3695.
- [39] A. Peterson, J. Nørskov, Activity descriptors for CO₂ electroreduction to methane on transition-metal catalysts, *J. Phys. Chem. Lett.* 3 (2012) 251–258.